3. 従来ソフトウェアと独自構築のパイプラインとの差異
4. エンドユーザーフレンドリー、患者フレンドリーなGUI開発
5. 研究班各施設からのゲノム情報解析ソフト開発に関する問い合わせについて

16:10 ～ 16:20

遺伝性心筋症パネル解析実施概要説明

東京大学大学院　医学系研究科　循環器内科学
野村　征太郎

1. 心筋症既知遺伝子パネル解析の現状と今後の方向性
2. 拠点班での解析のワークフロー

16:20 ～ 16:30

遺伝性不整脈パネル解析実施概要説明

滋賀医科大学　循環器内科学
大野　聖子

1. 不整脈既知遺伝子パネル解析の現状と今後の方向性
2. 拠点班での解析のワークフロー

16:30 ～ 16:50

症例収集概要説明、各学会との連携

国立循環器病研究センター　臨床研究部　心臓血管内科
北風　政史

1. 遺伝性循環器疾患の症例を統一したプロトコールで収集する意義
2. ゲノム解析に連結される最小限の臨床情報の蓄積
3. 将来目標：難病患者ネットワーク、各学会との連携協力
4. 倫理委員会申請が最初の共同作業、各施設での承認

＜配布資料＞

別紙１．ロードマップ

別紙２．全エクソン解析仕様

別紙３．情報解析仕様

別紙４．本研究で対象となる症例選択と解析選択、解析手順
（検体送付、授受、保存管理　システム）

＜解析に関する御相談、事務お問い合わせ先＞

厚生労働科学研究委託費（難治性疾患等実用化研究事業）
「遺伝性心血管疾患における集中的な遺伝子解析及び原因究明に関する研究」
研究代表者　　高島成二
事務局　　朝野仁裕（asano@cardiology.med.osaka-u.ac.jp）
科研事務担当秘書　岡田裕子（y-okada@cardiology.med.osaka-u.ac.jp）
〒 565-0871　大阪府吹田市山田丘 2-2　大阪大学大学院 医学研究科 医化学講座
ＴＥＬ：06-6879-3492、ＦＡＸ：06-6879-3493

別紙１．ロードマップ

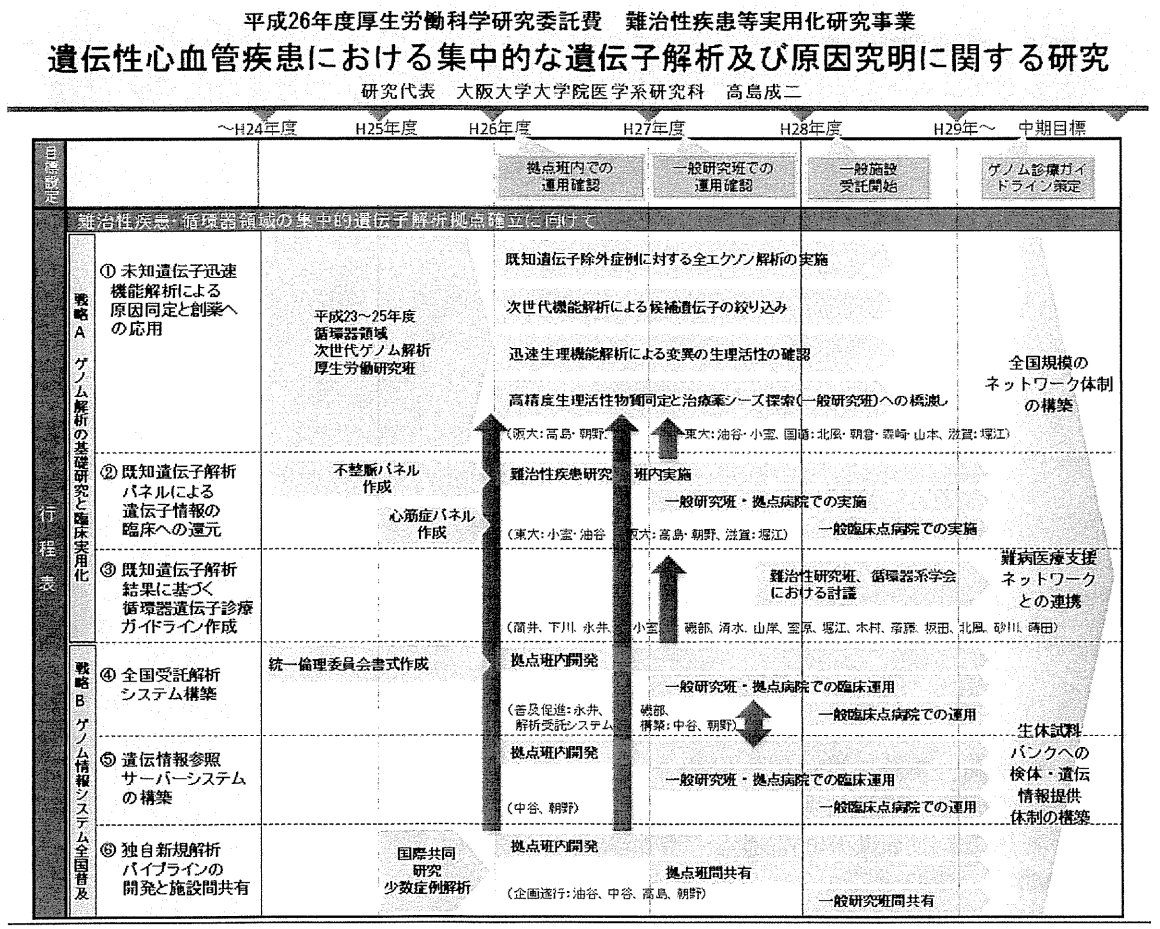
平成26年度厚生労働科学研究委託費　難治性疾患等実用化研究事業
遺伝性心血管疾患における集中的な遺伝子解析及び原因究明に関する研究
研究代表　大阪大学大学院医学系研究科　高島成二
～H24年度
H25年度
H26年度
H27年度
H28年度
H29年～
中期目標
自己評価
拠点班内での運用確認
一般研究班での運用確認
一般施設受託開始
ゲノム診療ガイドライン策定
難治性疾患・循環器領域の集中的遺伝子解析拠点確立に向けて
行程表
戦略A ゲノム解析の基礎研究と臨床実用化
戦略B ゲノム情報システム全国普及
① 未知遺伝子迅速機能解析による原因同定と創薬への応用
② 既知遺伝子解析パネルによる遺伝子情報の臨床への還元
③ 既知遺伝子解析結果に基づく循環器遺伝子診療ガイドライン作成
④ 全国受託解析システム構築
⑤ 遺伝情報参照サーバーシステムの構築
⑥ 独自新規解析パイプラインの開発と施設間共有
平成23～25年度 循環器領域 次世代ゲノム解析 厚生労働研究班
既知遺伝子除外症例に対する全エクソン解析の実施
次世代機能解析による候補遺伝子の絞り込み
迅速生理機能解析による変異の生理活性の確認
高精度生理活性物質同定と治療薬シーズ探索（一般研究班）への橋渡し
全国規模のネットワーク体制の構築
（阪大：高島・朝野、東大：油谷・小室、国循：北風・朝倉・森崎・山本、滋賀：堀江）
不整脈パネル作成
心筋症パネル作成
難治性疾患研究班内実施
一般研究班・拠点病院での実施
（東大：小室・油谷、阪大：高島・朝野、滋賀：堀江）
一般臨床点病院での実施
難病医療支援ネットワークとの連携
難治性研究班、循環器系学会における討議
（岡井、下川、永井、小室、磯部、清水、山岸、室原、堀江、木村、帯原、坂田、北風、砂川、諏訪）
統一倫理委員会書式作成
拠点班内開発
一般研究班・拠点病院での臨床運用
（普及促進：永井、解析受託システム：磯部、構築：中谷、朝野）
一般臨床点病院での運用
生体試料バンクへの検体・遺伝情報提供体制の構築
拠点班内開発
一般研究班・拠点病院での臨床運用
（中谷、朝野）
一般臨床点病院での運用
国際共同研究 少数症例解析
拠点班内開発
拠点班間共有
（企画遂行：油谷、中谷、高島、朝野）
一般研究班間共有

別紙２．全エクソン解析仕様

A　全エクソンキャプチャー
　　Agilent technology社　All Human Exon SureSelect V5+mtDNA

B　全エクソンシーケンシング
　　Illumina Hiseq 1000、2000、2500
　　100bp-PE解析
　　5000万リード/検体以上

（検体）
・検体種別　：　ゲノム DNA 溶液
・総量：10μg 以上
・濃度：100ng/μL 以上

1. サンプル品質を電気泳動および濃度測定により確認。
2. DNAライブラリーを作製。
3. SureSelect Human All Exon V5+mtDNA（Agilent）ターゲット領域の濃縮。
4. 濃縮DNAライブラリー6種を等量混合する。
5. 次世代シーケンサーHiSeq（Illumina）を用いて100base両末端シーケンスを実施
6. 合計5000万リード/検体相当のyield
   濃縮比較データ（on Target rate 90%（20×coverage））
   fastqファイルによる返却。
7. 6サンプル混合シーケンスの各検体あたりの取得データ量

C　ゲノム DNA 抽出は別枠で実施可能

別紙３．情報解析仕様

A　全国ネットワーク受託解析システムの研究開発
症例ゲノム情報（シーケンサが出力する FASTQ 形式ファイル）および付随する臨床情報を、大阪大学（最先端医療イノベーションセンター）に設置するデータストレージへ収載する。収載に当たっての症例 ID の付与や家系情報を含む臨床情報の入力、あるいは、症例 ID による病院施設から収載データを参照するためのシステムの構築に当たっては、新規ソフトウェアの開発を行うと共に、既存の商用の臨床研究・バイオバンク基盤ソフトウェアの活用を検討する。

B　遺伝情報参照サーバーシステムの研究開発
下記 C 項で開発するデータベース内の変異の情報を、セキュアな通信経路による配信、もしくは、ディスク等の外部メディアを介したデータコピーによって施設間で共有する仕組みを整備する。アクセス権に従って、変異および検体に関する情報をインタラクティブに閲覧できるデータベース検索システムを構築する。

C　新規解析パイプラインの開発と施設間共有システムの研究開発
下記の 3 段階から構成される解析パイプラインを大阪大学(最先端医療イノベーションセンター)に設置のサーバー上に構築する。1～2 では、標準的に用いられている公開ソフトウェア群を高スループットで実行する運用システムを構築する。3 では、1～2 で取得した変異から疾患検体もしくは疾患検体群に特異的な変異を抽出する新規手法の開発を行う。抽出した特異的な変異を収載したマスターデータベースを構築する。

1. FASTQ 形式ファイルから VCF 形式ファイルの生成（変異情報抽出）
2. VCF 形式ファイル内の変異の注釈付与とエクソン領域の絞り込み
3. 疾患関連変異の抽出

別紙４．本研究で対象となる症例選択と解析選択（案）

＜症例選択案＞

二次性心筋症が除外できている遺伝性を疑う心筋症（孤発症例を含む）
遺伝性を疑う不整脈疾患
その他遺伝性を疑う循環器疾患

※１　遺伝性心筋症、蓄積性心筋症、遺伝性不整脈、大動脈炎、原発性肺高血圧、等
※２　遺伝性（家族内発症）が疑われる循環器疾患症例
　　または　家族内罹患症例の採血ができず発端者のみの場合にも採血を実施
※３　病態が特殊な希少疾患、症候群に罹患した遺伝性を疑う症例

＜同定確率を上げる工夫・家系図作成・同意書取得範囲の目安＞

１）家系内では遠戚発症者をエントリーできる方が同定確率は高い
２）家系内の発症者は遠戚、近親にかかわらず基本的に全例取れる方が良い
３）発端者のみの解析の場合には両親の採血が必要（トリオ解析の実施）
　　特に、遺伝性か否かは不明も、症例が特殊で遺伝子の関与を疑う時
　　de novo mutation も想定し、トリオ解析を実施する

＜全エクソン解析と既知遺伝子パネル解析の解析実施基準＞

１）遺伝性心筋症、および遺伝性不整脈に該当するものは全例に拠点班において既知遺伝子パネル解析を実施する
２）全エクソン解析を実施について判断は、試料採取実施機関にて決定
３）全エクソン解析と既知遺伝子パネル解析ともに情報解析結果はDB化して拠点班の責任による保存管理を実施（拠点班内に情報を共有できるシステムを同時に構築）

＜全エクソン解析と既知遺伝子パネル解析の解析実施費用＞

解析順序：

Step1：ゲノムDNA抽出	各分担施設で負担
Step2：パネル解析	拠点で負担
Step3：全エクソン解析	各分担施設で負担
Step4：情報解析	拠点で負担

ワークフロー

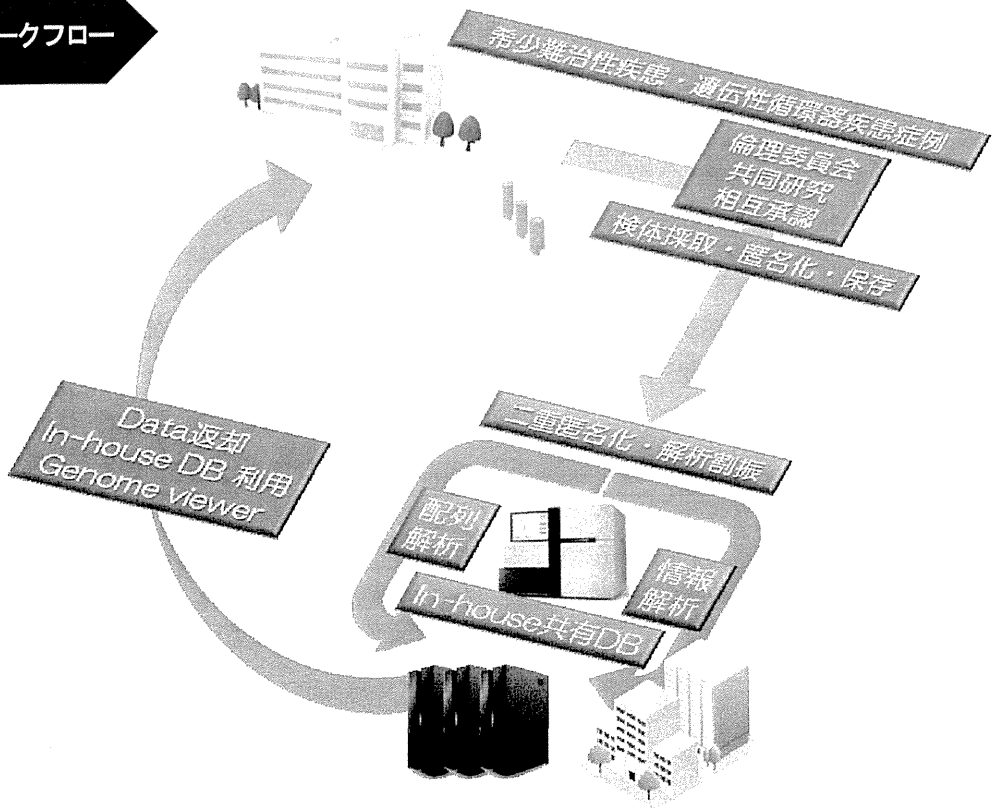
希少難治性疾患・遺伝性網膜脈絡膜疾患症例
倫理委員会
共同研究
相互承認
検体採取・匿名化・保存
二重匿名化・解析割振
配列
解析
情報
解析
In-house共有DB
Data返却
In-house DB 利用
Genome viewer

＜生体試料の種別＞

血液検体

EDTA-2K　紫スピッツ 2ml ×3 本

1 本は自施設にて保存、2 本を大阪大学へ送付・解析

ゲノム DNA 検体

全体収量が 10μg、濃度が 100ng/μl 以上が目安

＜全エクソン解析仕様＞

A　検体必要量

・検体種別 ： ゲノム DNA 溶液（ゲノム DNA 抽出は別枠で実施可能）

・総量：10μg 以上

・濃度：100ng/μL 以上

B　エクソンキャプチャー

Agilent technology社　All Human Exone SureSelect V5+mtDNA

C　シーケンシング

Illumina Hiseq 1000、2000、2500

100bp-PE解析

5000万リード/検体以上

1. サンプル品質を電気泳動および濃度測定により確認。
2. DNAライブラリーを作製。
3. Target enrichment：SureSelect Human All Exon V5+mtDNA（アジレント社）
4. 濃縮DNAライブラリー6種を等量混合する。
5. 次世代シーケンサーHiSeq（イルミナ社）を用いて100base両末端シーケンスを実施
6. 合計5000万リード/検体相当のyield

   濃縮比較データ（on Target rate 90%（20×coverage））

   fastqファイルによる返却。
7. 6サンプル混合シーケンスの各検体あたりの取得データ量

＜目標収集検体数＞

WES 解析：年間約 150～200 検体

パネル解析：年間約 300 検体

既知パネル費用は拠点分担施設負担（東大・滋賀医大）

Whole Exon Sequence（WES）解析費用：

NGS 解析費用（WES・DNA 抽出）は、各施設で実費負担

拠点班員からの解析依頼には統一価格で実施

「臨床検体サンプルに関する情報提供用紙」

[illegible]

1. 解析受託名称　[illegible]

2. 検体名　[illegible]

3. 検体性状　□ 血液　□ 血清・血漿

□ 組織

□ その他

4. 主な検体提供者　□ 健常人　□ 疾患患者　（疾患名）

5. 感染性の確認（必ずチェックしてください）

○ HBV, HCV, HIV感染の有無

□ 臨床検査で否定されている　□ 臨床所見から可能性は極めて低い　□ 関連する情報が無い

□ 感染が確認されている　（検査

○ その他感染症の感染の有無

□ 臨床所見から可能性は極めて低い　□ 関連する情報が無い

□ 感染が確認されている　（検査

6. その他、検体の収集方法など、サンプル中に感染性・病原性微生物等の存在を推測可能な情報がある場合、記載してください。

上記内容に相違ないことを保証します。

受託依頼者

ご所属

お名前　　印

ご連絡先（TEL/FAX）

ご記入日　　年　　月　　日

上記内容を確認後、弊社解析担当者から解析作業の可否をご連絡いたします。
ご依頼の内容によっては、弊社安全委員会での審議・承認にお時間を頂戴することがございますが、
何卒、ご理解のほどお願い申し上げます。
なお、弊社ではレベル3以上の微生物や安全性が確認できない検体は受け入れておりません。ご了承ください。

＜検体送付先＞

〒 565-0871　大阪府吹田市山田丘 2-2　大阪大学大学院 医学研究科 医化学講座
ＴＥＬ：06-6879-3492、ＦＡＸ：06-6879-3493
事務局宛

（参考資料２）登録管理システム

エキソーム解析受付

必要項目をご入力後「確認」ボタンを押してください

入力者の情報をご入力ください。　(情報共有者メールアドレスは任意項目)

診療科名 (倫理委員会計画書・講座名)　講座名をご選択ください

氏名

内線番号

メールアドレス

メールアドレス (確認)　@

パスワード (英数半角)

パスワード (確認)

情報共有者メールアドレス 1

情報共有者メールアドレス 2

情報共有者メールアドレス 3

検体情報をご入力ください。

依頼検体数 (半角数字)

解析優先度　申し込み順通り　至急解析を希望

匿名化 ID の下四桁 (半角数字)

想定遺伝形式　常染色体優性 AD　複合ヘテロ接合体変異 Compound hetero
常染色体劣性 AR　伴性劣性 X-linked　新規突然変異 de novo

提出検体情報　血液　組織　抽出済み

データバンク登録　可　不可

再解析同意　可　不可

Exome 解析エンリッチメントキット情報　SureSelectVer3　SureSelectVer4
SureSelectVer5　SureSelectVer5+mtDNA
その他

確認

大阪大学大学院医学系研究科 XXXX
お問い合わせ先: YYYY (内線 ZZZZ)

エキソーム解析受付

受付情報の送信処理中です。　■■ ■■ ■■ 受付情報の送信処理が完了しました。

エキソーム解析をご利用いただきましてありがとうございます。
aaaa@hoge.med.osaka-u.ac.jp からのメールをご確認ください。

Exome HP

大阪大学大学院医学系研究科 XXXX
お問い合わせ先: YYYY (内線 ZZZZ)

（参考資料 3）

（A）情報解析システムの構成概略

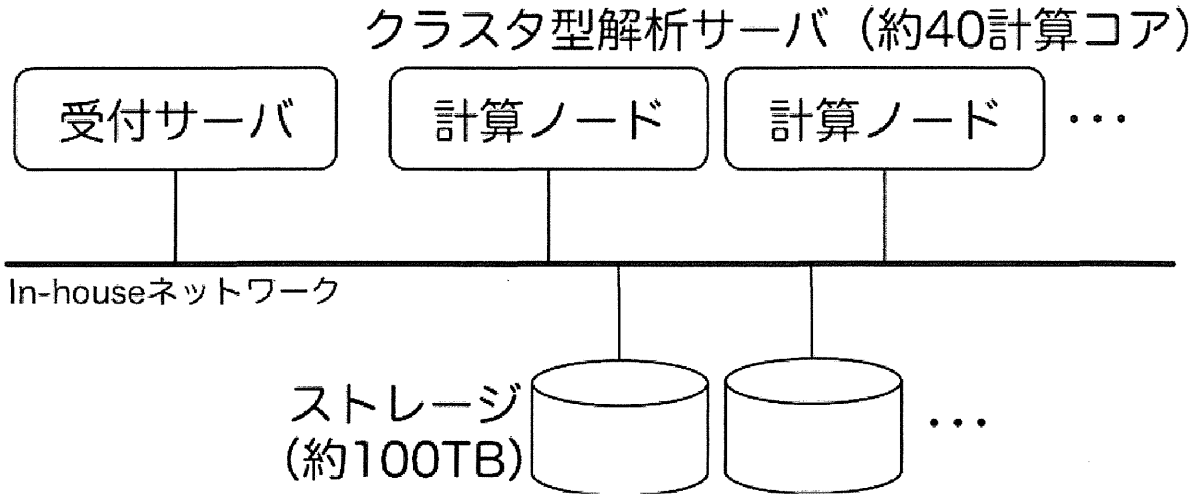

（B）シーケンサーデータの登録と情報表示

GIPL/JLS (Job Launching System)

ファイルを選択　2 ファイル　Upload

Subject	Batch ID	SureSelect	Mate1 (size,timestamp)			Mate2 (size,timestamp)		
A00001	1	V4	A00001_1.fastq	7.5GB	2015-03-03 05:19:52 (Tue)	A00001_2.fastq	7.5GB	2015-03-03 05:19:52 (Tue)
S00001	2	V4	S00001_1.fastq	7.5GB	2015-03-02 20:53:54 (Mon)	S00001_2.fastq	7.5GB	2015-03-02 20:53:54 (Mon)
S00002	3	V4	S00002_1.fastq	7.5GB	2015-03-10 21:09:18 (Tue)	S00002_2.fastq	7.5GB	2015-03-10 21:09:18 (Tue)
S00003	4	V4	S00003_1.fastq	7.5GB	2015-03-10 21:09:20 (Tue)	S00003_2.fastq	7.5GB	2015-03-10 21:09:20 (Tue)
S00004	5	V4	S00004_1.fastq	7.5GB	2015-03-10 21:09:21 (Tue)	S00004_2.fastq	7.5GB	2015-03-10 21:09:21 (Tue)
S00005	6	V4	S00005_1.fastq	7.5GB	2015-03-10 21:09:23 (Tue)	S00005_2.fastq	7.5GB	2015-03-10 21:09:23 (Tue)
S00006	7	V4	S00006_1.fastq	7.5GB	2015-03-10 21:20:21 (Tue)	S00006_2.fastq	7.5GB	2015-03-10 21:20:21 (Tue)

（参考資料 4）

（A）原因遺伝子同定ソフトウェアの実行中画面

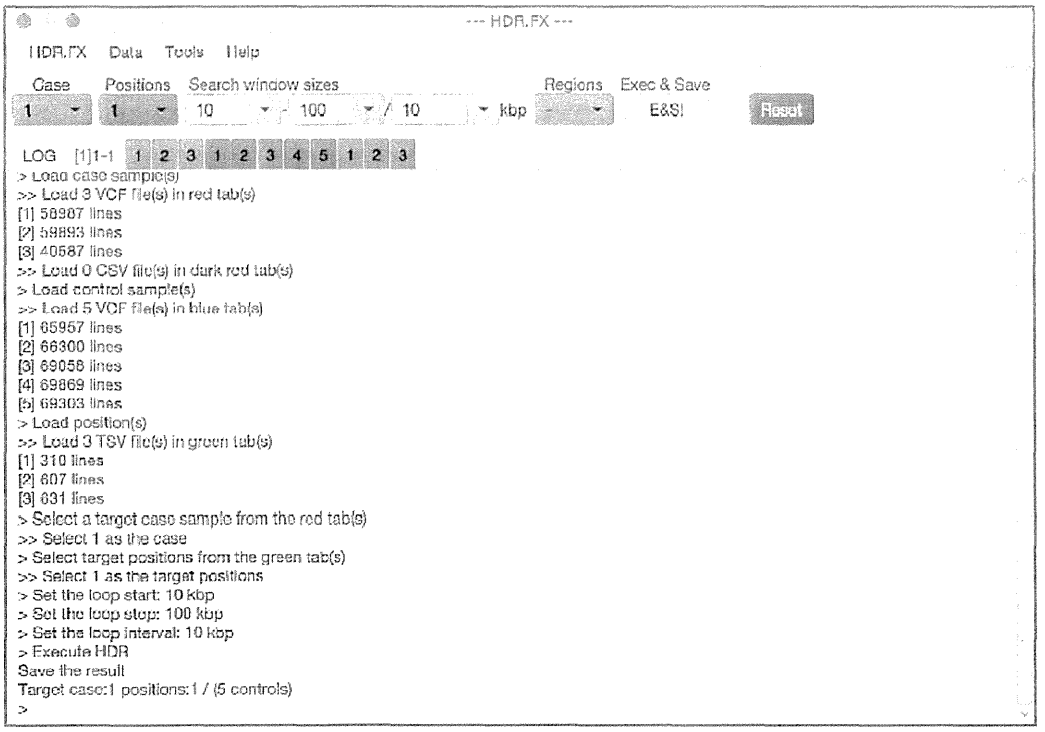

(B) 原因遺伝子同定ソフトウェアの情報ページ(概要とダウンロード)

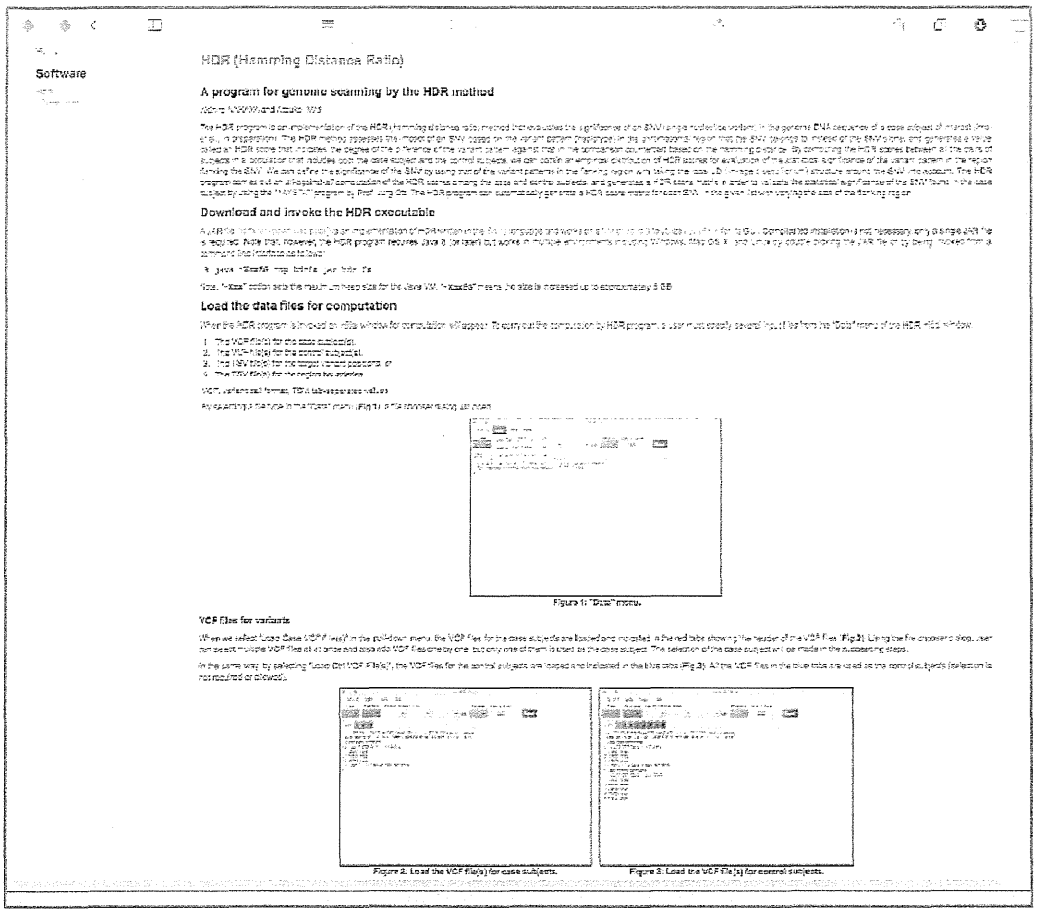

Software

HDR (Hamming Distance Ratio)

A program for genome scanning by the HDR method

Download and invoke the HDR executable

Load the data files for computation

VCF files for variants

Figure 1: "Data" menu.

Figure 2: Load the VCF file(s) for case subjects.

Figure 3: Load the VCF file(s) for control subjects.

Ⅳ. 研究成果の刊行物・別刷

Higd1a is a positive regulator of cytochrome *c* oxidase

Takaharu Hayashi[a,b], Yoshihiro Asano[a,b,1], Yasunori Shintani[a], Hiroshi Aoyama[c], Hidetaka Kioka[b], Osamu Tsukamoto[a], Masahide Hikita[d], Kyoko Shinzawa-Itoh[d], Kazuaki Takafuji[e], Shuichiro Higo[a,b], Hisakazu Kato[a], Satoru Yamazaki[f], Ken Matsuoka[b], Atsushi Nakano[g], Hiroshi Asanuma[h], Masanori Asakura[g], Tetsuo Minamino[b], Yu-ichi Goto[i], Takashi Ogura[d], Masafumi Kitakaze[g], Issei Komuro[j], Yasushi Sakata[b], Tomitake Tsukihara[d,k], Shinya Yoshikawa[d], and Seiji Takashima[a,k,1]

Departments of [a]Medical Biochemistry and [b]Cardiovascular Medicine, [e]Center for Research Education, and [c]Graduate School of Pharmaceutical Science, Osaka University Graduate School of Medicine, Suita, Osaka 565-0871, Japan; [d]Department of Life Science, University of Hyogo, 3-2-1 Kouto, Kamigohri, Akoh, Hyogo 678-1297, Japan; [k]Core Research for Evolutional Science and Technology (CREST), Japan Science and Technology Agency, Kawaguchi, Saitama 332-0012, Japan; Departments of [f]Cell Biology and [g]Clinical Research and Development, National Cerebral and Cardiovascular Center Research Institute, Suita, Osaka 565-8565, Japan; [h]Department of Cardiovascular Science and Technology, Kyoto Prefectural University School of Medicine, Kamigyo-ku, Kyoto 602-8566, Japan; [i]Department of Child Neurology, National Center Hospital of Neurology and Psychiatry, National Center of Neurology and Psychiatry, Kodaira, Tokyo 187-8502, Japan; and [j]Department of Cardiovascular Medicine, Graduate School of Medicine, University of Tokyo, Tokyo 113-8656, Japan

Edited by Gottfried Schatz, University of Basel, Reinach, Switzerland, and approved December 16, 2014 (received for review October 15, 2014)

Cytochrome *c* oxidase (CcO) is the only enzyme that uses oxygen to produce a proton gradient for ATP production during mitochondrial oxidative phosphorylation. Although CcO activity increases in response to hypoxia, the underlying regulatory mechanism remains elusive. By screening for hypoxia-inducible genes in cardiomyocytes, we identified *hypoxia inducible domain family, member 1A* (*Higd1a*) as a positive regulator of CcO. Recombinant Higd1a directly integrated into highly purified CcO and increased its activity. Resonance Raman analysis revealed that Higd1a caused structural changes around heme *a*, the active center that drives the proton pump. Using a mitochondria-targeted ATP biosensor, we showed that knockdown of endogenous Higd1a reduced oxygen consumption and subsequent mitochondrial ATP synthesis, leading to increased cell death in response to hypoxia; all of these phenotypes were rescued by exogenous Higd1a. These results suggest that Higd1a is a previously unidentified regulatory component of CcO, and represents a therapeutic target for diseases associated with reduced CcO activity.

cytochrome *c* oxidase | oxidative phosphorylation | resonance Raman spectroscopy | ATP | oxygen

Cytochrome *c* oxidase (CcO) (ferrocytochrome c: oxygen oxidoreductase, EC 1. 9. 3. 1) is the terminal component of the mitochondrial electron transfer system. CcO couples the oxygen-reducing reaction with the process of proton pumping. Aerobic organisms use this reaction to form a proton gradient across the mitochondrial inner membrane, which is ultimately used by the F_oF_1-ATP synthase to produce ATP.

Mammalian CcO is composed of 13 different subunits (1) containing four redox-active metal centers, two copper sites, and two heme *a* groups. These active centers accept electrons from cytochrome *c* and sequentially donate them to dioxygen. Our group and others have extensively analyzed the link between the oxygen reduction process and proton pumping at the active centers using crystallography, resonance Raman spectroscopy, and Fourier transform infrared spectroscopy (2–4). The metal ions in the copper sites and heme groups in the active centers are individually coordinated by the surrounding amino acids. We have shown that changes in the redox state cause 3D structural changes around the active centers, which in turn leads to alteration of the proton pump mediated by specific amino acid chains that coordinate each metal group (5). Thus, binding of an allosteric regulator close to the active centers might change the efficiency of both electron transfer to oxygen and proton pumping.

Several proteins involved in oxygen supply or metabolism are transcriptionally regulated by intracellular oxygen concentration: vascular endothelial growth factor (VEGF) (6), erythropoietin (EPO) (7), and G0/G1 switch gene 2 (G0s2) for F_oF_1-ATP synthase, as we recently revealed (8). Because CcO is the only enzyme in the body that can use oxygen for energy transduction, it has been suggested that the regulatory mechanism of CcO is dependent on oxygen concentration (9–12); however, this has yet to be demonstrated. In this study, we aimed to identify a regulator of CcO driven by low oxygen concentration.

In this study, by screening for hypoxia-inducible genes, we discovered that *hypoxia inducible domain family, member 1A (Higd1a)* is a positive regulator of CcO. Furthermore, using our recently established ATP-sensitive fluorescence resonance energy transfer (FRET) probe, we demonstrated that Higd1a increased mitochondrial ATP production. We also showed that Higd1a directly bound CcO and changed the structure of its active center.

Results

***Higd1a* Expression Is Induced Early in the Response to Hypoxia.** During the first few hours of hypoxia, CcO and oxidative phosphorylation (OXPHOS) activity is activated, presumably to fully use any remaining oxygen (12). At later time points, metabolism shifts toward glycolysis. Therefore, we hypothesized that a positive regulator of CcO must be up-regulated during an early stage of hypoxia, but down-regulated when glycolysis-related genes become elevated. To identify early hypoxia responsive genes that

Significance

We identified hypoxia-inducible domain family, member 1A (Higd1a) as a positive regulator of cytochrome *c* oxidase (CcO). CcO, the terminal component of the mitochondrial electron transfer system, reductively converts molecular oxygen to water coupled to pump protons across the inner mitochondrial membrane. Higd1a is transiently induced under hypoxic conditions and increases CcO activity by directly interacting with CcO in the vicinity of its active center. Induction of Higd1a leads to increased oxygen consumption and subsequent mitochondrial ATP synthesis, thereby improving cell viability under hypoxia.

Author contributions: Y.A., Y. Shintani, H. Kioka, T.T., S. Yoshikawa, and S.T. designed research; T.H., Y. Shintani, H. Kioka, O.T., M.H., K.S.-I., K.T., and H. Kato performed research; H. Aoyama, M.H., Y.-i.G., T.O., M.K., I.K., Y. Sakata, T.T., and S. Yoshikawa contributed new reagents/analytic tools; T.H., Y. Shintani, S.H., S. Yamazaki, K.M., A.N., H. Asanuma, M.A., and T.M. analyzed data; and T.H., Y. Shintani, H. Kato, T.O., T.T., S. Yoshikawa, and S.T. wrote the paper.

The authors declare no conflict of interest.

This article is a PNAS Direct Submission.

[1]To whom correspondence may be addressed. Email: takasima@cardiology.med.osaka-u.ac.jp or asano@cardiology.med.osaka-u.ac.jp.

This article contains supporting information online at www.pnas.org/lookup/suppl/doi:10.1073/pnas.1419767112/-/DCSupplemental.

might regulate CcO activity, we analyzed gene-expression profiles of neonatal rat cardiomyocytes, one of the most mitochondria-rich cell types, exposed to hypoxic conditions (1% oxygen for 0, 4, or 12 h). Focusing on the genes whose expression was induced more than two-fold at 4 h relative to the prestimulation stage, but then decreased by 12 h, we identified three genes (Fig. 1*A* and Fig. S1 *A* and *B*). Next, we prioritized genes that were (*i*) well conserved among eukaryotes and (*ii*) listed in MitoCarta (13); only one gene, *Higd1a*, satisfied both criteria. To analyze the endogenous expression levels of Higd1a in rat cardiomyocytes, we raised a specific antibody against Higd1a and confirmed its specificity (Fig. S2 *A* and *B*). In cardiomyocytes exposed to hypoxia, Higd1a protein levels increased gradually from 0 to 12 h and then decreased by 24 h (Fig. 1*B*). Immunofluorescence revealed that both endogenous and exogenous Higd1a localized in the mitochondria (Fig. S2*C*).

Higd1a Directly Integrates into the CcO Macromolecular Complex. Because Rcf1a, the yeast homolog of Higd1a, associates with CcO (9–11), we first tested whether mammalian Higd1a binds to CcO in vivo. Indeed, endogenous binding between Higd1a and CcO in rat cardiomyocytes was confirmed by immunocapture with an anti-Higd1a antibody (Fig. S3*A*) and verified by reciprocal coimmunoprecipitation with an anti-Cox4 antibody (Fig. S3*B*). This in vivo interaction was further validated by blue native PAGE (BN-PAGE) of mitochondrial fractions from rat cardiomyocytes (Fig. S3*C*).

Because preparation of the CcO macromolecular complex, which consists of 13 subunits, is technically demanding, it has remained unclear whether Rcf1a/Higd1a binding to CcO is direct. To address this issue, we performed an in vitro pull-down assay using highly purified bovine CcO (hpCcO), which we prepared by dissolving microcrystals used for X-ray structural analysis (14). Notably, recombinant maltose binding protein-fused bovine Higd1a (MBP-Higd1a) (Fig. S4) directly associated with hpCcO (Fig. 1*C*). Furthermore, to assess macromolecular complex formation, we performed BN-PAGE followed by immunoblotting with an antibody against Higd1a, demonstrating that recombinant Higd1a indeed integrated into hpCcO (Fig. 1*D*). With these results, we conclude that Higd1a directly associates and integrates into the CcO macromolecular complex.

Higd1a Causes Structural Changes in CcO and Influences the Active Center of Heme *a*. To explore the relevance of the interaction between Higd1a and CcO, we investigated whether recombinant Higd1a affects hpCcO enzymatic activity. Strikingly, direct addition of MBP-Higd1a to hpCcO significantly increased CcO activity to twice that of hpCcO alone or hpCcO mixed with MBP (Fig. 2*A*). This significant increase in hpCcO activity stimulated by Higd1a led us to speculate that Higd1a causes a structural change at the active centers of CcO.

Therefore, we next investigated whether Higd1a changes the intensity of the visible part of the absorption spectrum of oxidized CcO. MBP alone, used as a negative control, did not cause a significant change in the absorption spectra (Fig. S5). By contrast, MBP-Higd1a caused significant spectral changes at 413 nm and 432 nm (Fig. 2*B*), wavelengths that reflect conformational changes around the hemes in oxidized CcO (15).

To obtain further structural insights, we performed resonance Raman spectroscopy, a powerful and sensitive method for detecting kinetic structural changes that cannot be assessed by X-ray crystal structural analysis. Fig. 2*C* depicts the resonance Raman spectra of CcO with and without MBP-Higd1a, focusing on the heme structure by using 413 nm excitation. The resonance Raman band at 1,372 cm^{-1} in (a: hpCcO) and (b: hpCcO + Higd1a) is assignable to the ν_4 mode of heme and is indicative of ferric heme. After the addition of recombinant Higd1a, the resonance Raman spectra demonstrated two sets of different peaks (or band shifts) at 1,562/1,592 cm^{-1} (the ν_2 mode; a marker for the spin state of heme) (16) and 1,673/1,644 cm^{-1} (the $\nu_{CH=O}$ mode of the formyl group of heme *a*) (17). Importantly, the frequency shift of the band at 1,592 cm^{-1} to 1,562 cm^{-1} is attributable to partial conversion of heme from a low-spin to a high-spin state. In oxidized CcO, only heme *a* includes low-spin iron; therefore, heme *a*, but not heme a_3, is responsible for the band shift (16). These data suggest that the binding of Higd1a to CcO caused structural changes at heme *a*, the active center of CcO.

Higd1a Positively Regulates CcO Activity and Subsequent Mitochondrial OXPHOS. Next, we investigated whether Higd1a truly regulates CcO activity in vivo. To this end, we assessed biochemical CcO activity in rat cardiomyocytes with modified expression of Higd1a. Notably, we observed a significant decrease in CcO activity in Higd1a knockdown cells. This effect was rescued by overexpression of Higd1a, eliminating the possibility of off-target effects in the RNAi experiment (Fig. 3*A*, *Left*). Moreover, overexpression of Higd1a alone increased the basal CcO activity (Fig. 3*A*, *Right*). These data suggest that Higd1a is an endogenous and positive regulator of CcO.

To assess the effect of Higd1a on cellular respiration, we continuously measured the oxygen consumption rate (OCR) using a XF96 Extracellular Flux Analyzer (Seahorse Bioscience).

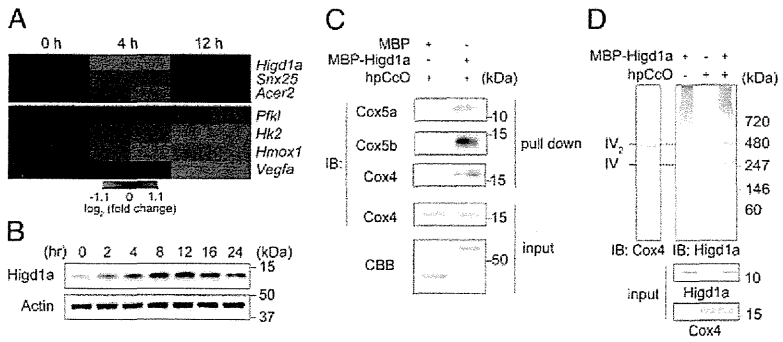

Fig. 1. Hypoxia-inducible Higd1a directly binds to highly purified cytochrome *c* oxidase (hpCcO). (*A*) Heat map of three genes (*Upper*) identified as relatively rapid and transiently induced in response to hypoxia in rat neonatal cardiomyocytes, compared with genes known to be hypoxia inducible (*Pfkl*, *Hk2*, *Hmox1*, and *Vegfa*) (*Lower*). (*B*) Expression of the Higd1a protein was elevated in response to hypoxia. (*C*) In vitro pull-down assay with amylose resin revealed direct binding between MBP-Higd1a and the hpCcO from bovine heart. Loading controls for the hpCcO and MBP-fusion proteins are shown in immunoblots for anti-CcO subunits and CBB staining, respectively. (*D*) MBP-Higd1a directly integrates into hpCcO. Mixed MBP-fusion proteins and hpCcO containing 0.2% *n*-decyl-β-D-maltoside (DM) were resolved by blue native PAGE (BN-PAGE), followed by immunoblotting with anti-Cox4 to detect CcO and anti-Higd1a to detect Higd1a.

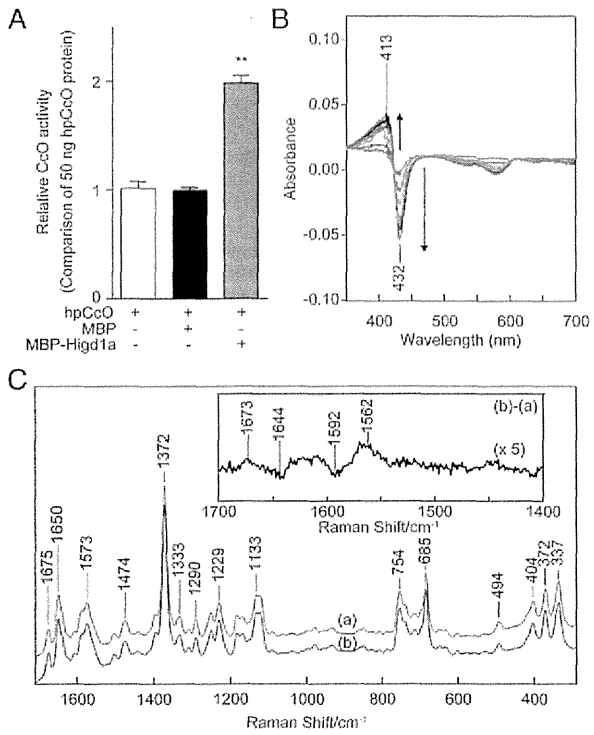

Fig. 2. Higd1a regulates CcO activity through the structural change of the active center in CcO. (*A*) CcO activity of hpCcO and hpCcO with either recombinant MBP or recombinant MBP-Higd1a. MBP-Higd1a causes an increase in CcO activity by almost twofold. Data represent the means ± SEM of five individual experiments. $^{**}P < 0.01$, compared with MBP. (*B*) The difference in absorption spectra between MBP-Higd1a and oxidized hpCcO. MBP-Higd1a caused spectral changes at 413 and 432 nm. Intensity changes of oxidized hpCcO spectra are plotted at 1 min (red), 5 min (brown), 10 min (dark yellow), 15 min (green), 20 min (light blue), 25 min (blue), and 30 min (purple) after adding MPB-Higd1a. (*C*) Resonance Raman spectra of oxidized hpCcO at 0–5 min [spectrum (a)] and oxidized hpCcO mixed with MBP-Higd1a at 0–5 min [spectrum (b)]. The *Inset* shows the difference of the spectra [(b) − (a)].

Knockdown of Higd1a caused a significant decrease in both basal (Fig. S6*A*, *Left*) and maximum OCR, and these effects were rescued by exogenous expression of Higd1a (Fig. 3*B*, *Left*). Moreover, overexpression of Higd1a significantly increased both basal and maximum OCR (Fig. S6*A*, *Right* and Fig. 3*B*, *Right*).

Because the electron transport chain creates a proton gradient that drives F_oF_1-ATP synthase (complex V), ATP production is the overall outcome of mitochondrial OXPHOS. To determine whether modulation of CcO activity by Higd1a affects ATP production, we performed the mitochondrial activity of streptolysin O permeabilized cells (MASC) assay, a sensitive means of measuring the mitochondrial ATP production rate in semi-intact cells (18). Indeed, Higd1a knockdown caused a significant decrease in the ATP production rate relative to the control (Fig. 3*C*), whereas overexpression of Higd1a increased it (Fig. 3*D*). These results suggest that Higd1a modulates mitochondrial OXPHOS through CcO.

Higd1a Protects Cardiomyocytes Under Hypoxic Conditions by Increasing ATP Production. We reasoned that endogenous induction of Higd1a by hypoxia serves to maintain ATP production in mitochondria to the greatest extent possible when oxygen supply is limited. The intramitochondrial matrix ATP concentration ($[ATP]_{mito}$) reflects mitochondrial ATP production far more sensitively than the cytosolic ATP concentration (8). Therefore, we next assessed the effect of Higd1a on ATP production in living cells using the FRET-based mitochondrial ATP biosensor Mit-ATeam (19). First, we examined the effect of KCN, an inhibitor of CcO. KCN significantly reduced the $[ATP]_{mito}$ (Fig. S7), suggesting that Mit-ATeam provides an effective means to monitor the functional consequences of changes in CcO activity. We then confirmed that hypoxia caused a gradual decline in $[ATP]_{mito}$. Overexpression of Higd1a alleviated the decline in $[ATP]_{mito}$ during hypoxia, whereas knockdown of Higd1a accelerated the decrease in $[ATP]_{mito}$ relative to the control (Fig. 4*A*).

The yeast homolog Rcf1 plays a role in respiratory supercomplex stability, and the same is true for Higd2a, but not Higd1a (11). We investigated whether Higd1a affects respiratory supercomplex stability Higd1a-knockdown or -overexpressing cells. As shown in Fig. S8, there was no significant change in the abundance or composition of the respiratory supercomplex, suggesting that the effect of Higd1a described above is not a result of changes in supercomplex stability.

Finally, to test whether the effects of Higd1a on mitochondrial ATP synthesis affected overall cell viability, we analyzed the viability of cardiomyocytes subjected to hypoxia. Under hypoxic conditions, Higd1a-knockdown cells showed a significant increase in cell death, and this effect was rescued by exogenous expression of Higd1a (Fig. 4*B* and Fig. S9*A*). In addition, overexpression of Higd1a alone

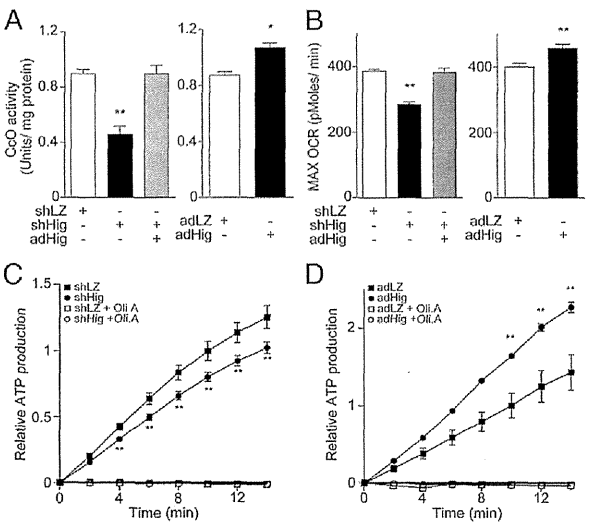

Fig. 3. Higd1a positively modulates mitochondrial respiration by altering CcO activity. (*A*, *Left*) Mitochondrial fraction from rat cardiomyocytes expressing shLacZ (shLZ), shHigd1a (shHig), or both shHig and adHigd1a (adHig) were subjected to the CcO activity assay. (*Right*) CcO activity was measured in cardiomyocytes treated with either adLacZ (adLZ) or adHig. Data represent the means of four individual experiments. (*B*, *Left*) The maximum oxygen consumption rate (max OCR) in rat cardiomyocytes transfected with the indicated adenovirus was measured after treatment with oligomycin A and fluorocarbonyl cyanide phenylhydrazone (FCCP). Knockdown of Higd1a resulted in a significant decrease in max OCR, which was rescued by exogenously expressed Higd1a. (*Right*) Overexpression of Higd1a significantly increased max OCR compared with the cells with adLZ ($n = 20$ for each group). (*C*) The relative ATP production rate of cardiomyocytes treated with shLZ or shHig was measured by the MASC assay ($n = 6$). A numerical value of ATP production at 10 min in shLZ groups is regarded as 1.0. (*D*) The relative ATP production rate of cardiomyocytes treated with adLZ or adHig was measured by MASC assay ($n = 5$). A numerical value of ATP production at 10 min in adLZ groups is regarded as 1.0. Data represent the means ± SEM; $^{*}P < 0.05$, $^{**}P < 0.01$.

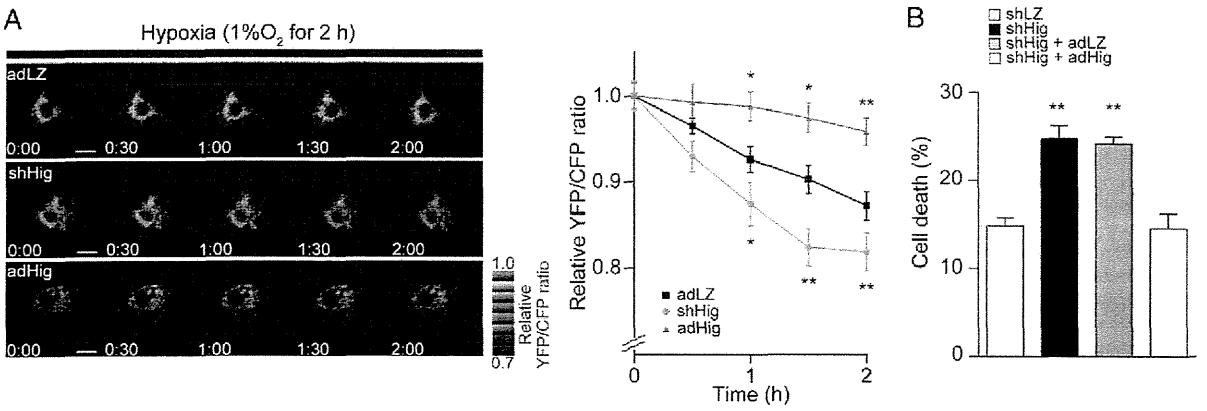

Fig. 4. (*A*) Representative sequential YFP/CFP ratiometric images of Mit-ATeam fluorescence in cardiomyocytes expressing corresponding adenovirus during hypoxia ($n = 12$ for adLZ, $n = 23$ for shHig, $n = 18$ for adHig). All of the measurements were normalized to the ratio at time 0 and compared between adLZ and adHig or shHig. (Scale bar, 20 μm.) (*B*) Cell death of cardiomyocytes treated with shHig was significantly increased compared with the control, which was rescued by addition of adHig under hypoxic conditions for 24 h ($n = 12$ for each group). Data represent the means of three independent cultures, ± SEM; $*P < 0.05$, $**P < 0.01$, compared with control (adLZ or shLZ).

increased cellular tolerance to hypoxia (Fig. S9*B*). On the basis of these findings, we conclude that Higd1a positively regulates CcO activity and subsequently increases mitochondrial ATP production, thereby protecting cardiomyocytes against hypoxia.

Discussion

In this study, we demonstrated that recombinant Higd1a produced in *Escherichia coli* was incorporated into CcO complex purified from bovine heart. The data suggest that Higd1a directly bound to the already assembled CcO complex and increased its activity. Together with the fact that Higd1a expression was rapidly increased by hypoxia, this observation indicated that Higd1a is a positive regulator of CcO that preserves the proton-motive force under hypoxic cellular stress. Physiologically, Higd1a preserved ATP production in healthy cardiomyocytes under hypoxic conditions, which protected them from an energy crisis leading to cell death.

We demonstrated that Higd1a incorporated into the CcO complex and increased its activity. It remains unclear which part of CcO is essential for this change. Higd1a binding may affect the interaction of cytochrome *c* with CcO, modulate internal electron/proton transfer, or modify K_d/K_m for O_2 binding to Cu_B/heme a_3. In fact, the resonance Raman spectroscopy experiment provided us with a clue to this question. First, we discovered that Higd1a markedly shifted the maximum Soret peak around 413 nm absorption, suggesting the occurrence of structural changes in heme that are usually observed during the reduction and oxidation process of CcO. This shift in absorbance prompted us to perform resonance Raman analysis at 413 nm excitation, a powerful tool for investigating the structure of heme and its vicinity. Higd1a induced a frequency shift of the band at 1,592 cm^{-1} to 1,562 cm^{-1} and 1,673/1,644 cm^{-1}; the former frequency is attributed to partial conversion of heme from a low-spin to a high-spin state. In oxidized CcO, only heme *a* includes low-spin iron (16); therefore, heme *a*, but not heme a_3, is responsible for this band shift.

X-ray structural and mutational analyses for bovine heart CcO have demonstrated that protons are pumped through the hydrogen-bond network across the CcO molecule, designated the H pathway, located near heme *a* (20). The driving force for active proton transport is electrostatic repulsion between the proton in the hydrogen-bond network and the net positive charge of heme *a*. One of the critical sites for repulsion is the formyl group of heme *a*, which is hydrogen bonded to Arg38 of the CcO subunit I (21). In our study, resonance Raman spectroscopy revealed specific band shifts from 1,644 cm^{-1} to 1,673 cm^{-1}, which can be attributed to the vibration of the formyl group of heme *a*. This observation suggests that Higd1a binding causes structural changes, particularly around heme *a*, weakening the hydrogen bond between the formyl group and Arg38 of the CcO subunit I, thereby leading to the acceleration of proton pumping efficiency (22). Thus, both band shifts suggest that structural change occurs in the vicinity of heme *a* rather than a_3.

Following the resonance Raman analysis, we sought to determine the Higd1a-CcO binding site via simulation with the COOT software (23), using the previously reported structures of CcO (14) and Higd1a (24). From our structural analysis, CcO contains a cleft composed of relatively few protein subunits near the active centers (Fig. S10*A*). Notably, Higd1a was predicted to integrate into the cleft of CcO near heme *a* and Arg38 (Fig. S10), consistent with the

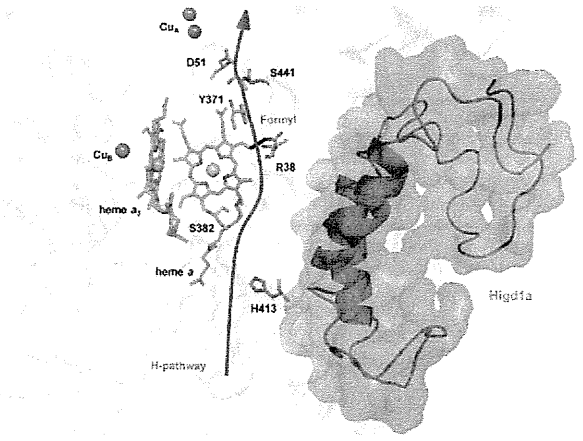

Fig. 5. Higd1a acts on the H pathway. Model depicting our docking simulation (side view) and its relationship with the H pathway. The model shows the location of Higd1a (magenta) in the CcO complex (white) and its relationship to R38 of cytochrome *c* oxidase subunit I and the formyl group of heme *a*, a component of the H pathway (red arrow).

results of the resonance Raman analysis. Thus, it is likely that Higd1a bound to the cleft of CcO, leading to swift structural change around heme *a* and Arg38 and accelerating the proton-pumping H pathway, thereby increasing CcO activity (Fig. 5). Furthermore, when we retrospectively reviewed the purification process of the CcO complex, comprising 13 subunits from the bovine heart, we found that Higd1a remained associated with CcO up to the final step, which required detergent exchange (14). This led us to speculate that Higd1a represents a 14th identified subunit of CcO that is endogenously induced by hypoxia and integrates into the open cleft of CcO to positively regulate its activity. Although the resonance Raman data and docking model simulation are consistent with the idea that Higd1a binding causes structural change around heme *a*, these data are limited because of their speculative nature. Therefore, to confirm these findings, we are currently trying to crystallize the CcO-Higd1a complex to reveal the conformational changes of CcO, particularly around the heme *a* site.

Higd1a was originally identified as a mitochondrial inner membrane protein whose expression is induced by hypoxia (25). Higd1a augments cell survival under hypoxic stress in pancreatic cells (26), and it exerts its protective effect by induction of mitochondrial fission (27). The precise relationship between these reports and our data is not clear. However, our results suggest that the elevation of CcO activity by Higd1a preserves the proton-motive force, which is prerequisite for mitochondria function, thereby leading to increased mitochondrial fission and/or the prevention of apoptosis.

The existence of a direct CcO allosteric activator suggests that there is a structural basis for the intrinsic activation in the CcO complex. To explore this idea further, a screen for small compounds that simply increase the activity of highly purified CcO in vitro has been initiated. Compounds that mimic the effect of Higd1a can preserve ATP production even under hypoxic condition, and hence are expected to exert cellular protective effects particularly when OXPHOS activity is reduced. Recent work showed that lowering the activity of OXPHOS causes the cellular senescence (28), diabetes mellitus (29), and neurodegenerative diseases (30). In addition, several currently intractable mitochondrial diseases are caused by mutations in mitochondrial genes or nuclear genes that lead to dysfunction in mitochondrial OXPHOS. Notably, decreased CcO activity is most frequently observed among patients with mitochondrial diseases (31). Therefore, small compounds that mimic the effect of Higd1a will have therapeutic potential for various acute and chronic diseases including ischemic, metabolic, and mitochondrial diseases.

Materials and Methods

Purification of Recombinant Higd1a Protein. The full-length bovine *Higd1a* cDNA was purchased from GE Healthcare. Then the coding sequence of bovine *Higd1a* was cloned in-frame with an ATG start codon, in the pET21a expression vector (Novagen for overexpression in *E. coli*). A MBP was fused in-frame at the amino terminus for purification. The resulting plasmid was transformed into BL21-Star (DE3; Invitrogen), and the addition of 0.5 mM isopropyl β-D-1-thiogalactopyranoside caused the expression of MBP-Higd1a protein. The cells were sonicated and solubilized by 1% *n*-decyl-β-D-maltoside (DM). The recombinant protein was purified with amylose resin (New England Biolabs), and eluted by 20 mM maltose (pH 6.8 or 8.0, 100 mM sodium phosphate buffer containing 0.2% DM). The eluted protein was concentrated and maltose removed using Amicon Ultra-0.5 10K (Millipore).

Resonance Raman Spectroscopy. Absorption spectra of the samples were measured by a spectrophotometer (Hitachi, U3310) with the path length of 2 mm in 100 mM sodium phosphate buffer (pH 8.0) containing 0.2% DM. The reaction mixture was measured immediately and spectra were recorded every 5 min for 30 min. The protein concentration was 8 μM.

Raman scattering of the samples were measured in a cylindrical spinning cell with excitation at 413.1 nm with a Kr^+ laser (Spectra Physics, model 2060), and the incident power was 500 μW. The detector was a liquid N_2-cooled CCD detector (Roper Scientific, Spec-10: 400B/LN). Raman shifts were calibrated with indene as the frequency standard. Raman spectrum was divided by the "white light" spectrum that was determined by measuring the scattered radiation of an incandescent lamp by a white paper to compensate for the sensitivity difference of each CCD pixel and transmission curve of the notch filter to reject Rayleigh scattering. The accuracy of the peak position of well-defined Raman bands was ±1 cm^{-1}. The protein concentration was 20 μM, and the reaction mixture was incubated for 30 min, before Raman measurements.

Measurement of CcO Activity. CcO activity was measured spectrophotometrically (Shimazu, UV-2450) using a cytochrome *c* oxidase activity kit (Biochain). A total of 25 μg of mitochondrial pellets from cardiomyocytes was lysed with 1% *n*-dodecyl-β-D-maltoside (DDM), and subjected to measurement according to the manufacturer's instructions (32). Concentrations of reduced/oxidized cytochrome *c* were determined using the extinction coefficient at 550 nm of 21.84 $mM^{-1}cm^{-1}$. For in vitro measurement, cytochrome *c* (Sigma) was reduced by ascorbic acid (Wako). Recombinant MBP-Higd1a (20 μM) and hpCcO (20 μM) were incubated at 25 °C for 30 min in the presence of 0.2% DM. After incubation, the mixture and reduced cytochrome *c* were added into the assay buffer, then subjected to measurement at 30 °C (Agilent Technologies, cary300). Slopes of OD_{550} for 1 min were calculated and corrected by a value of hpCcO.

FRET-Based Measurement of Mitochondrial ATP Concentration. FRET-based measurement of mitochondrial ATP concentration in cardiomyocytes was measured as previously described (8, 33). Briefly, FRET signal was measured in cardiomyocytes infected with adenovirus encoding mit-AT1.03 with an Olympus IX-81 inverted fluorescence microscope (Olympus) using a PL APO 60×, 1.35 N.A., oil immersion objective lens (Olympus). Fluorescence emission from Mit-ATeam was imaged by using a dual cooled CCD camera (ORCA-D2; Hamamatsu Photonics) with a dichroic mirror (510 nm) and two emission filters (483/32 nm for CFP and 542/27 nm for YFP; A11400-03; Hamamatsu Photonics). Cells were illuminated using the CoolLED pE-1 excitation system (CoolLED) with a wavelength of 425 nm. Image analysis was performed using MetaMorph (Molecular Devices). The YFP/CFP emission ratio was calculated by dividing pixel by pixel (a YFP image with a CFP image after background subtraction).

Statistical Analyses. The comparison between two groups was made by *t* test (two tailed). For MASC assay, comparison was made by repeated two-way ANOVA. A value of $P < 0.05$ was considered statistically significant. Data represent mean ± SEM.

Further methods are found in *SI Materials and Methods*.

ACKNOWLEDGMENTS. We thank T. Miyazaki (Cyclex) for making antibodies; Y. Okazaki and Y. Tokuzawa (Saitama Medical University) for measurement of CcO activity by cary300; Dr. Steven Coppen for critical reading of the manuscript; S. Ikezawa, E. Takada, and H. Shingu for technical assistance; M. Kobayashi, R. Maki, and the Center for Research Education in Osaka University for MS analysis; Y. Okada for secretarial support; and H. Shimada for discussion and advice. This research was supported by the Japan Society for the Promotion of Science through the "Funding Program for Next Generation World-Leading Researchers (NEXT Program)," initiated by the Council for Science and Technology Policy; grants-in-aid from the Ministry of Health, Labor, and Welfare-Japan; grants-in-aid from the Ministry of Education, Culture, Sports, Science, and Technology-Japan; and grants-in-aid from the Japan Society for the Promotion of Science. This research was also supported by grants from Takeda Science Foundation, Japan Heart Foundation, Japan Cardiovascular Research Foundation, Japan Intractable Diseases Research Foundation, Japan Foundation of Applied Enzymology, Japan Medical Association, Uehara Memorial Foundation, Mochida Memorial Foundation, Banyu Foundation, Naito Foundation, Inoue Foundation for Science, Osaka Medical Research foundation for intractable diseases, Ichiro Kanehara Foundation, and Showa Houkoukai.

1. Tsukihara T, et al. (1996) The whole structure of the 13-subunit oxidized cytochrome c oxidase at 2.8 A. *Science* 272(5265):1136–1144.
2. Morgan JE, Vakkasoglu AS, Lanyi JK, Gennis RB, Maeda A (2010) Coordinating the structural rearrangements associated with unidirectional proton transfer in the bacteriorhodopsin photocycle induced by deprotonation of the proton-release group: A time-resolved difference FTIR spectroscopic study. *Biochemistry* 49(15):3273–3281.
3. Aoyama H, et al. (2009) A peroxide bridge between Fe and Cu ions in the O2 reduction site of fully oxidized cytochrome c oxidase could suppress the proton pump. *Proc Natl Acad Sci USA* 106(7):2165–2169.
4. Ogura T, Kitagawa T (2004) Resonance Raman characterization of the P intermediate in the reaction of bovine cytochrome c oxidase. *Biochim Biophys Acta* 1655(1-3): 290–297.